❑ Data and Preliminary Results

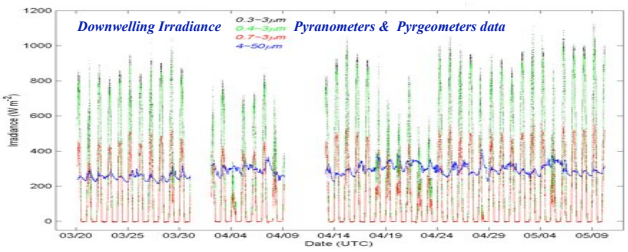

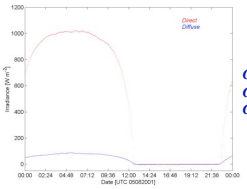

Clean & Cloud-free Conditions

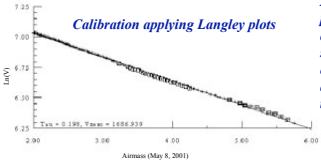

Aerosol optical thickness retrievals from shadowband radiometer or sunphotometer data

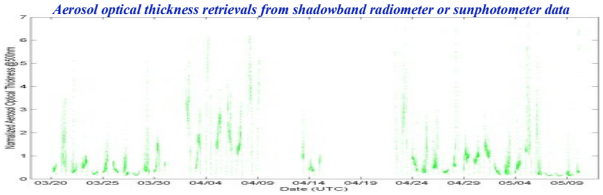

Aerosol Radiative Forcing Efficiency:

$$\frac{\partial T}{\partial t} = \frac{-1}{C_p \rho}\frac{\partial F_{net}}{\partial z} \propto \frac{\Delta F_{net}}{\Delta \tau}$$

The atmospheric warming/cooling rates (e.g., near surface) are proportional to the aerosol radiative forcing efficiency which is defined as the change of net irradiance due to the change of the aerosol optical thickness (i.e., cloud-free).

After cloud screening, all irradiance data are plotted against the aerosol optical thickness data. For a given airmass, the slope of the scatter plot is the corresponding forcing efficiency – the amount of irradiance altered due to a change of unit aerosol optical thickness.

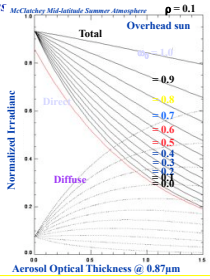

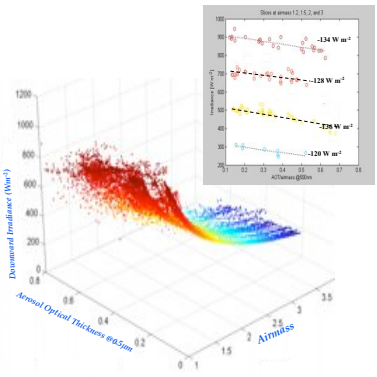

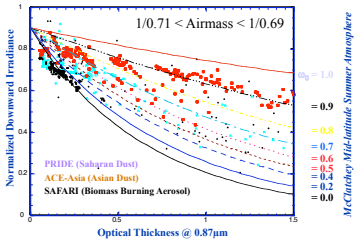

Data to be used for investigating the microphysical, optical, and radiative properties of dust:

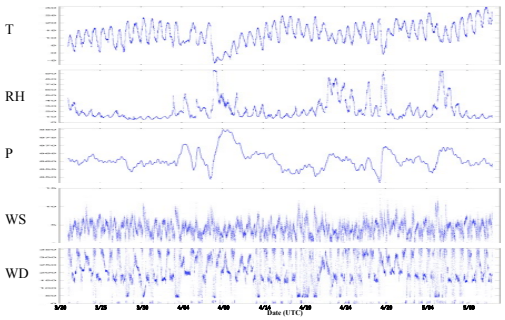

- *A diurnal cycle is clearly observed from data collected by these meteorological sensors.*
- *The local relative humidity is usually low, however increased relative humidity and some precipitation is associated with synaptic systems.*
- *The highest wind speed observed was about 15 m/sec during the April 28 dust storm.*
- *Due to the topography, wind direction changes from easterly to westerly as the day progresses.*

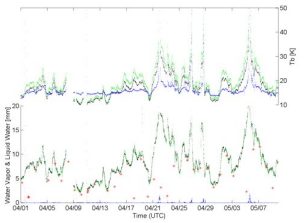

Atmospheric column water vapor and liquid water can be inferred from brightness temperature measurements at frequencies of 23.0, 23.8 and 36.5 GHz. Two pairs of frequencies, (23.0, 36.5) and (23.8, 36.5) GHz applied to the tipping curve calibration, are used in the retrieval algorithm. The Terra/MODIS product of daytime column water vapor (, 10:30 AM overpass) is compared. The results retrieved from both microwave and solar channels agree very well, except those with clouds (ice or water, based on lidar data) which affect the solar retrievals (above cloud amount).*

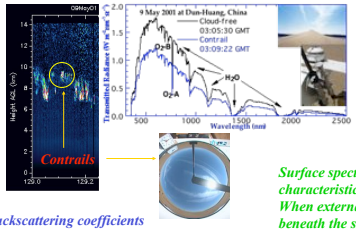

Transmitted solar spectra, before and during a contrail blocking the sun, were acquired under relatively clean sky conditions with six contrails at different aging stages. Molecular absorption bands are clearly revealed.

Nephelometer

The particle sizer and the nephelometer were overwhelmed by the high dust concentration. Nevertheless, a few comparisons among differing dust conditions are presented.

Particle sizer

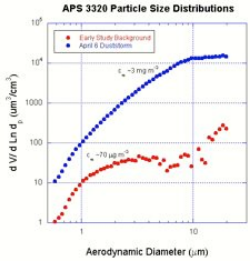

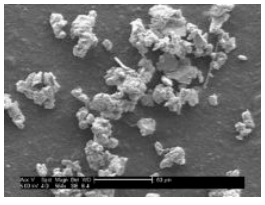

At the Dun-Huang site, micrograph depicts a dust predominately of silicates, with additional clay minerals, carbonates, feldspars and gypsum (M. Dunlap, Dept. of Chemical Engineering and Material Science, UC Davis).

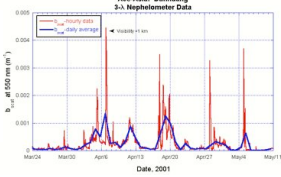

Aerosol backscattering coefficients measured at three visible wavelengths show the temporal characteristics of five major dust events at the Dun-Huang site.

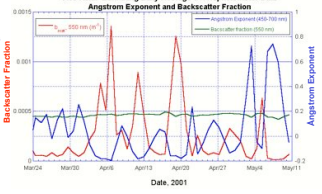

Surface spectral albedo measurements show characteristics of the composite sand and small gravel. When external force is applied, the gravel is forced beneath the sand, which alter the spectral albedo.